the plant journal

SEB Society for Experimental Biology

The Plant Journal (2017) **92,** 1092–1105 doi: 10.1111/tpj.13745

An Arabidopsis divergent pumilio protein, APUM24, is essential for embryogenesis and required for faithful pre-rRNA processing

Thiruvenkadam Shanmugam[1,†], Nazia Abbasi[1,†], Hyung-Sae Kim[1], Ho Bang Kim[1,‡], Nam-il Park[1,§], Guen Tae Park[2], Sung Aeong Oh[3], Soon Ki Park[3], Douglas G. Muench[4], Yeonhee Choi[2], Youn-Il Park[5] and Sang-Bong Choi[1,*]

[1]*Division of Bioscience and Bioinformatics, Myongji University, Yongin Kyunggi-do 449-728, South Korea,*
[2]*School of Biological Sciences, Seoul National University, Seoul 151-747, South Korea,*
[3]*School of Applied Biosciences, Kyungpook National University, Daegu 702-701, South Korea,*
[4]*Department of Biological Sciences, University of Calgary, Calgary, AB, T2N 1N4, Canada, and*
[5]*Department of Biological Sciences, Chungnam National University, Daejeon 305-764, South Korea*

Received 15 December 2016; revised 28 September 2017; accepted 3 October 2017; published online 14 October 2017.
*For correspondence (e-mail choisb@mju.ac.kr).
†T.S. and N.A. contributed equally to this work.
‡Present address: Biomedic Co., Ltd., Bucheon, Kyunggi-do, 420-852, South Korea.
§Present address: Department of Plant Science, Gangneung-Wonju National University, Gangneung, Gangwan-do, 210-702, South Korea.

SUMMARY

Pumilio RNA-binding proteins are largely involved in mRNA degradation and translation repression. However, a few evolutionarily divergent Pumilios are also responsible for proper pre-rRNA processing in human and yeast. Here, we describe an essential Arabidopsis nucleolar Pumilio, APUM24, that is expressed in tissues undergoing rapid proliferation and cell division. A T-DNA insertion for *APUM24* did not affect the male and female gametogenesis, but instead resulted in a negative female gametophytic effect on zygotic cell division immediately after fertilization. Additionally, the mutant embryos displayed defects in cell patterning from pro-embryo through globular stages. The mutant embryos were marked by altered auxin maxima, which were substantiated by the mislocalization of PIN1 and PIN7 transporters in the defective embryos. Homozygous *apum24* callus accumulates rRNA processing intermediates, including uridylated and adenylated 5.8S and 25S rRNA precursors. An RNA–protein interaction assay showed that the histidine-tagged recombinant APUM24 binds RNA *in vitro* with no apparent specificity. Overall, our results demonstrated that APUM24 is required for rRNA processing and early embryogenesis in Arabidopsis.

Keywords: APUM24, *Arabidopsis thaliana*, embryogenesis, nucleolus, Puf RNA-binding protein, RNA–protein interaction, rRNA processing.

INTRODUCTION

Post-transcriptional regulation of gene expression plays an important role during growth and development, and includes RNA splicing, editing, capping, polyadenylation, RNA transport, stability and translation (Okita and Choi, 2002; Belostotsky and Sieburth, 2009; Barkan and Small, 2014; Cheng *et al.*, 2016). Most of these processes are achieved either directly or indirectly by RNA-binding proteins (Lorkovic, 2009; Marondedze *et al.*, 2016). Pumilio (Puf) proteins are a group of highly conserved eukaryotic RNA-binding proteins that possess characteristic Puf domains (Bailey-Serres *et al.*, 2009; Abbasi *et al.*, 2010; Tam *et al.*, 2010). Puf proteins participate in rRNA processing, mRNA stability and translation, and thereby control embryonic development, stem cell maintenance and neurogenesis (Spassov and Jurecic, 2003; Abbasi *et al.*, 2010; Miller and Olivas, 2011; Quenault *et al.*, 2011; Qiu *et al.*, 2014; Gennarino *et al.*, 2015; Naudin *et al.*, 2017). They usually possess an RNA-binding domain that contains eight tandem Puf repeats, of which each repeat is 35–39 amino acids in length, and typically bind to 8-nt sequences in the 3′-untranslated region (UTR) of target mRNAs. Puf target RNAs contain a highly conserved UGUA core motif flanked by less conserved AU-rich sequences (Zamore *et al.*, 1997; Wharton *et al.*, 1998; Gerber *et al.*, 2004). Each Puf repeat binds to a single RNA base using a specificity code that involves three key amino acids located on the

second α-helix of each Puf repeat (Wang *et al.*, 2002; Campbell *et al.*, 2014). Although Puf proteins fold into a crescent-shaped structure and bind to RNAs with sequence specificity (Dong *et al.*, 2011; Filipovska *et al.*, 2011; Yosefzon *et al.*, 2011), a recent study revealed that human Puf-A and yeast Puf6 show an L-shaped structure and bind to RNA in a sequence-independent manner (Qiu *et al.*, 2014).

Two Pumilio proteins (Arabidopsis APUM5 and APUM23) have been characterized in detail thus far in plants (Abbasi *et al.*, 2010; Huh *et al.*, 2013; Huang *et al.*, 2014). APUM23 is a nucleolar protein that is required for rRNA processing (Abbasi *et al.*, 2010; Huang *et al.*, 2014), whereas cytoplasmic APUM5 suppresses cucumber mosaic virus (CMV) infection via direct binding to a specific 3′-UTR sequence of CMV RNA 1 (Huh *et al.*, 2013). An *apum23* mutant accumulated 35S pre-rRNA, unprocessed 18S rRNA and polyadenylated 5.8S pre-rRNA, indicating that APUM23 plays a role in the degradation of rRNA maturation byproducts. APUM23 binds to non-canonical consensus elements with a central UUGA core (Zhang and Muench, 2015). Besides these two Pumilio proteins, although its binding substrate has not been examined, APUM9 was known to be involved in reduced seed dormancy that is closely related with APUM10 and APUM11 in the gene and protein structure (Xiang *et al.*, 2014).

In Arabidopsis, three Pumilios (APUM23, APUM24 and APUM25) are evolutionarily diverging members out of 25 on the basis of their amino acid conservation and the location of Puf domains (Francischini and Quaggio, 2009). In this study, we show that APUM24 is a nucleolar protein essential for embryogenesis. In the absence of *APUM24*, embryos failed to develop beyond the globular stage, and accumulated uridylated 27SB and the 3′-extended 5.8S pre-rRNA including polyadenylated byproducts. Further, APUM24 bound to 5.8S and ITS2 region in a sequence-independent manner. Our finding suggests that APUM24 is required for timely removal of rRNA byproducts for rapid cell division and precise embryonic patterning.

RESULTS

APUM24 is a nucleolar protein expressed in actively proliferating cells

Puf domains of APUM24 protein are interspersed throughout the entire sequence, unlike typical Puf proteins in which tandem repeat Puf domains are located on the C-terminal half (Spassov and Jurecic, 2003; Francischini and Quaggio, 2009; Tam *et al.*, 2010). Phylogenetic analysis and localization prediction demonstrated that APUM24 is closely related to the nucleolar yeast Puf6 and human Puf-A proteins (Figure S1), suggesting a nucleolar function such as rRNA processing (Qiu *et al.*, 2014). To examine the subcellular localization of APUM24, *35S:GFP-APUM24* and *35S:APUM24-GFP* constructs were transformed transiently into tobacco (*Nicotiana benthamiana*) leaves and stably into Arabidopsis plants. Transient assays in tobacco leaves showed that APUM24 is a nucleolar protein (Figure S2a). Consistently, stably expressed GFP-APUM24 localized to the nucleolus but did not target to Cajal bodies (Figure 1a). A similar localization pattern was also observed for APUM24-GFP plants that co-expressed AtCoilin-mRFP (Figure S2b).

We next examined the tissue expression of *APUM24* using quantitative real-time-polymerase chain reaction (qRT-PCR) in wild-type, and using *APUM24:APUM24-GFP* and *APUM24:GUS* transgenics. A qRT-PCR and GUS histochemical analysis showed that *APUM24* is expressed in all tissues examined with lower levels in older leaves (Figures 1b and S3). Similarly, APUM24-GFP expression under the *APUM24* promoter was also observed in all tissues, with higher levels in rapidly dividing cells and expanding tissues, including young primary and lateral root cells, pollen mother cells and dividing ovule cells (Figure 1c, upper panels). During embryogenesis, APUM24-GFP was detected in the endosperm and all stages of the embryo, but absent in the suspensor by the late heart stage (Figure 1c, bottom panels). These results indicate that APUM24 is expressed in all tissues undergoing active growth and cell division.

A previous microarray study demonstrated that *APUM24* is a sugar-responsive gene that is upregulated by 3.86-fold at 4 h after glucose supplementation (Li *et al.*, 2006). Therefore, we examined the expression level of *APUM24* in wild-type Col-0 seedlings treated with glucose or sucrose using qRT-PCR (Figure 1d). Expression was induced within 30 min and remained high up to 6 h. Glucose supplementation stimulated GUS expression in the vascular tissues and cell division zone containing the apical meristem of primary roots in *APUM24:GUS* plants (Figure 1e).

Mutation of *APUM24* results in a defect in seed setting

To gain insight into the function of APUM24, we next examined three mutant alleles for *APUM24*, namely *apum24-1*, *apum24-2* and *apum24-3* (Figure 2a). Other than possessing shrunken seeds, *apum24-2*$^{-/-}$ plants did not exhibit any morphological difference as compared with wild-type plants (Figure 2b). No homozygous mutants were obtained for *apum24-1* and *apum24-3* alleles, but instead heterozygous plants set both normal and the aborted ovules or seeds, which were completely rescued by the genomic DNA containing the entire *APUM24* gene (Figure 2c; Tables S1 and S2). When seeds of the *apum24-1*$^{+/-}$ and *apum24-3*$^{+/-}$ plants were germinated on the selection medium, they showed a non-Mendelian segregation ratio (Table S2). The atypical segregation ratio of *apum24-1* and *apum24*-3 raised the possibility that there were defects in male and/or female gametogenesis. To test this

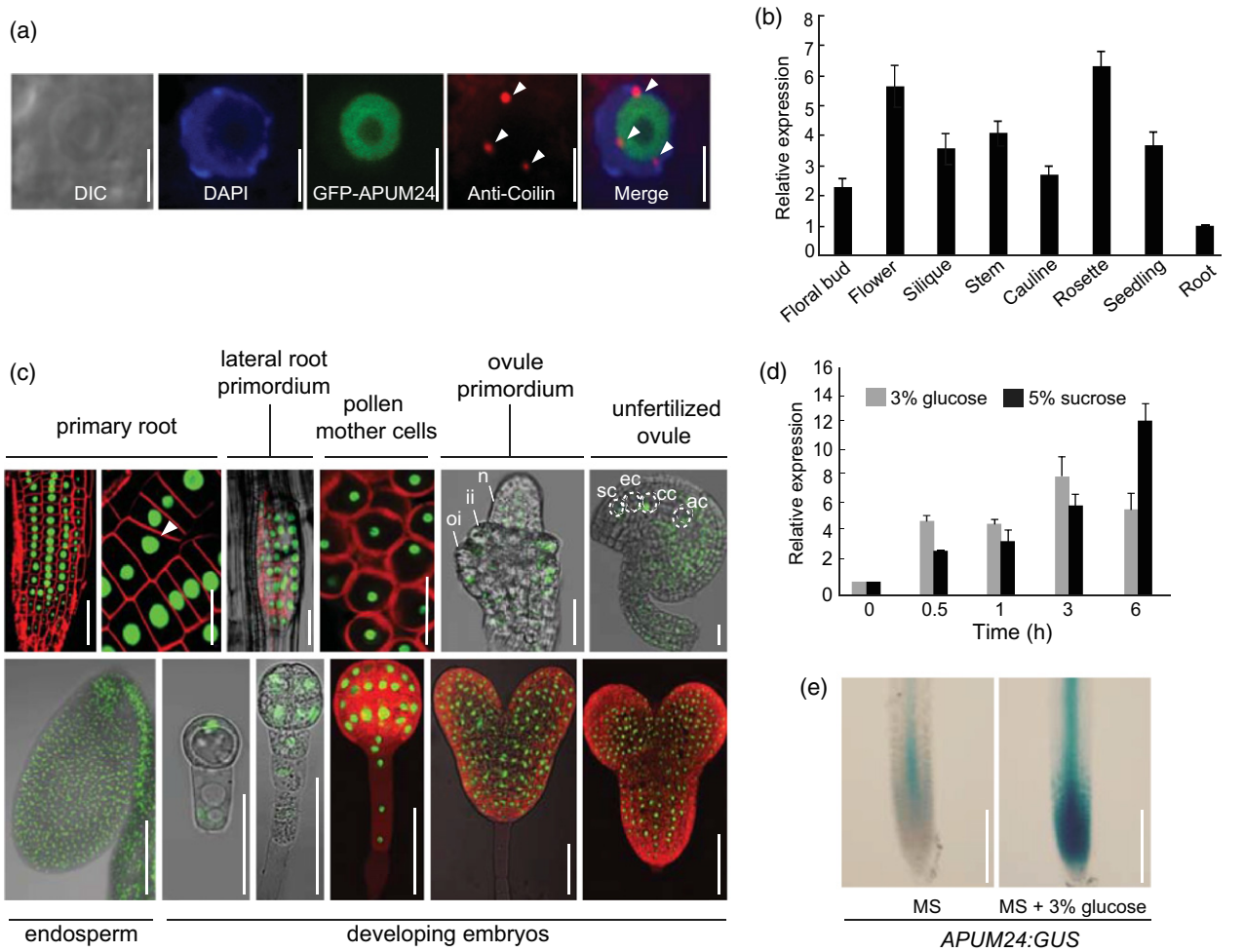

Figure 1. Nucleolar localization of GFP-APUM24 and tissue-specific expression of *APUM24*.
(a) Localization of a GFP-APUM24 fusion protein in root cells of transgenic Arabidopsis. GFP signal is localized in the nucleolus but not in Cajal bodies (arrowheads). Cajal body immunofluorescence was detected using AtCoilin antibody. DIC, differential interference contrast image. Scale bars: 50 μm.
(b) Quantitative real-time-polymerase chain reaction (qRT-PCR) analysis of *APUM24* expression in wild-type Col-0 seedlings.
(c) Confocal images of *APUM24:APUM24-GFP* expression in various tissues. Ten-day-old transgenic plants were used for observations of GFP expression in primary and lateral roots and 2-day-old seeds after pollination in the endosperm. The cell membrane was visualized by FM4-64 stain (red). n, nucellus; ii, inner integument; oi, outer integument; ac, antipodal cell; cc, central cell; ec, egg cell; sc, synergid cell. Scale bars: 50 μm.
(d) Sugar-mediated upregulation of *APUM24* mRNA in 1-week-old seedlings grown on MS medium.
(e) Increased GUS expression in the root of 10-day-old *APUM24:GUS* plants in the presence of 3% glucose. Scale bars: 100 μm. [Colour figure can be viewed at wileyonlinelibrary.com].

possibility, we performed a reciprocal cross between *apum24-1*$^{+/-}$ and wild-type plants (Table S3), and found that *apum24-1* is defective in female gametogenesis and/or has a deleterious maternal effect on embryogenesis. Because *apum24-2* was a leaky mutant (Figure 2b) and *apum24-3*$^{+/-}$ showed similar segregation ratio with *apum24-1*$^{+/-}$, *apum24-1* allele was selected for further study.

Mutation of *APUM24* does not affect gametogenesis

To see if *apum24-1* is defective in male and female gametogenesis, we examined the division patterns of pollen and ovule cells using GFP markers. Mature pollen from *apum24-1*$^{+/-}$ plants was fertile and viable (Figure S4), and their sperm cells and vegetative nuclei have undergone normal development as visualized by DAPI staining (Figure S5; Table S4) and by the expression of the sperm cell marker (*H3.3:H3.3-mRFP1*; Ingouff *et al.*, 2007) or a vegetative and sperm cell marker (*SCP:H2B-mRFP*; Oh *et al.*, 2010) in the *apum24-1*$^{+/-}$ *qrt1-4*$^{-/-}$ plants (Figures 2d and S6; Table S5). The *apum24-1*$^{+/-}$ plant was crossed with GFP marker lines for the following ovule identity cells: antipodal cells (*DD1:GFP*); synergid cells (*DD2:GFP*); central cells (*DD7:GFP*); and egg cells (*DD45:GFP*; Steffen *et al.*, 2007; Figure S7; Table S6). No defect in female gametogenesis was observed. In addition, the ovules in *apum24-1*$^{+/-}$

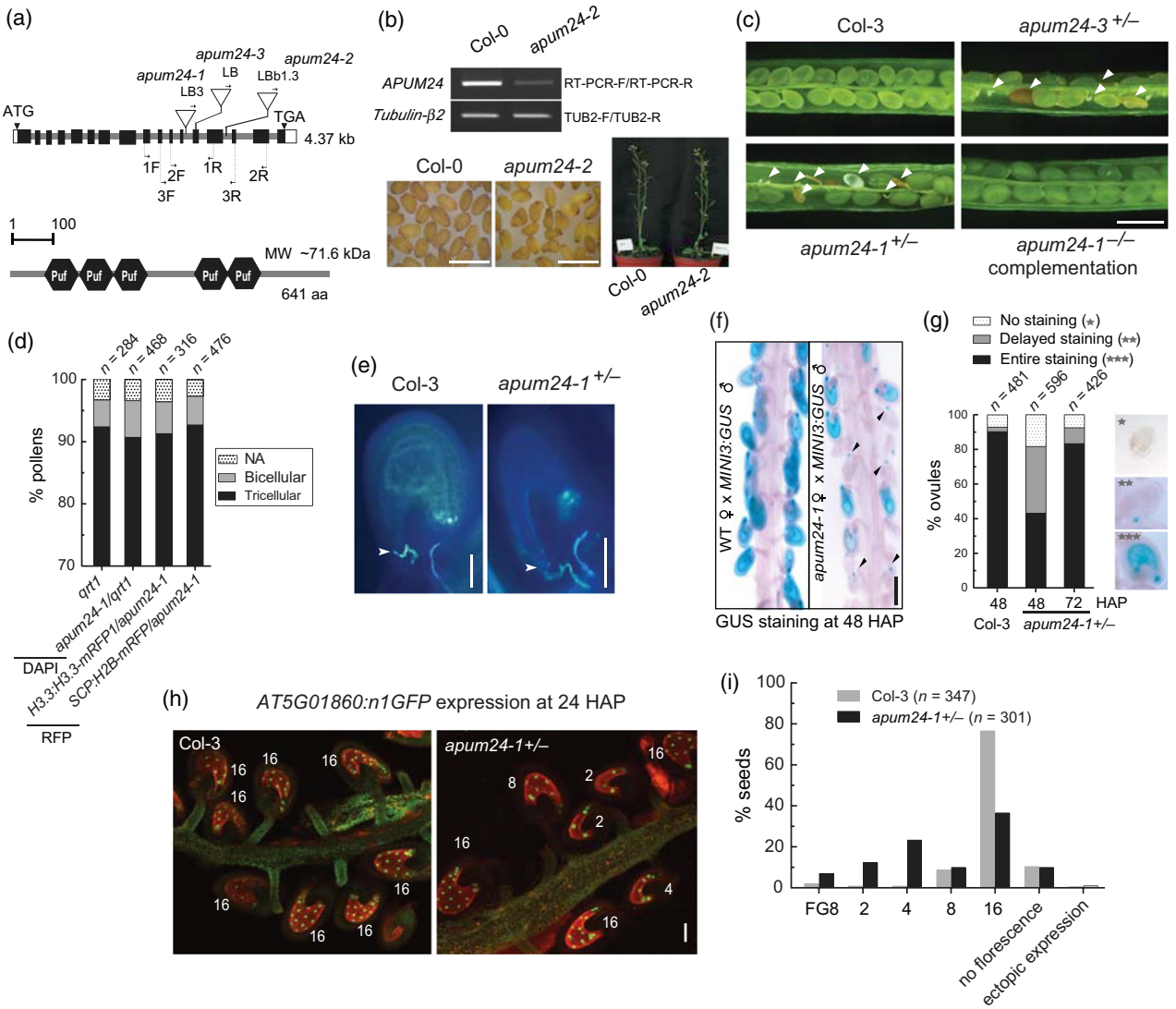

Figure 2. *APUM24* is essential for seed setting and its mutation delays cell division after fertilization.
(a) T-DNA insertion locations of *apum24* mutant alleles. The black boxes indicate coding exons and blank boxes untranslated exons. The primers used for genotyping are indicated with arrows (Table S9). Primary structure of APUM24 with 5 Puf domains is shown in the bottom.
(b) Phenotypes of *apum24-2*$^{-/-}$ seeds and mature plant. RT-PCR shows a low level of *APUM24* expression. Scale bars: 0.5 mm.
(c) Open siliques of *apum24-1*$^{+/-}$, *apum24-3*$^{+/-}$ and *apum24-1*$^{-/-}$ plants complemented with CAMBIA1301-APUM24-6K construct containing the wild-type *APUM24* gene. Aborted seeds are shown with white arrowheads. Scale bar: 1 mm.
(d) Percent of pollen at the bicellular and tricellular stages of anthesis in wild-type and *apum24-1*$^{+/-}$ plants in the *qrt1* mutant background. Sperm and vegetative nuclei were counted using DAPI stain, the sperm cell nuclear marker (*H3.3:H3.3-mRFP1*), or the sperm cell and vegetative nuclear marker (*SCP:H2B-mRFP*). NA, aborted pollens.
(e) Pollen tube growth towards the micropylar end (arrowheads) of Col-3 and *apum24-1* ovules. Ovules were stained with aniline blue. Scale bars: 50 μm.
(f) GUS staining of wild-type and *apum24-1*$^{+/-}$ seeds expressing *MINI3:GUS* at 48 h after pollination (HAP). GUS expression was observed in the entire endosperm and in the majority of fertilized seeds in wild-type plants, but was variable in *apum24-1*$^{+/-}$ seeds and often restricted to a small area (seen as small puncta) in slow-growing seeds with asynchronous development (black arrowheads). Scale bar: 200 μm.
(g) Quantitative GUS staining patterns as described in (f) at 48 and 72 HAP with no staining (*), delayed staining (**) and entire endosperm staining (***). Note that at 72 HAP, *apum24-1*$^{+/-}$ seeds expressed GUS at similar levels to wild-type seeds.
(h) *At5g01860:n1GFP* expression in wild-type and *apum24-1*$^{+/-}$ seeds at 24 HAP. Wild-type seeds are in the 16-cell endosperm stage, whereas heterozygous mutant seeds are asynchronous in the 2- to 16-cell stages. Scale bar: 20 μm.
(i) Asynchrony in endosperm cell divisions in seeds from the *apum24-1*$^{+/-}$ at 24 HAP. Data were obtained from the siliques when wild-type endosperm reaches the 16-cell stage. [Colour figure can be viewed at wileyonlinelibrary.com].

flowers were competent to attract pollen tubes (Figures 2e and S8). Hence, the abnormal segregation pattern of self-fertilized *apum24-1*$^{+/-}$ (and the reciprocal cross) was not due to defective male and/or female gametogenesis. This raised the possibility of a female gametophytic effect on post-gametophytic development.

apum24 mutant ovules show delayed fertilization

We next determined fertilization efficiencies by pollinating the pistils of wild-type and *apum24-1*$^{+/-}$ plants with pollen from homozygous *MINI3:GUS* plants (Luo *et al.*, 2005). The *MINI3* gene encodes the transcription factor WRKY10. It is often used as a marker for fertilization as GUS protein is expressed in the developing endosperm from the two nuclei stage at ~12 h post-fertilization to endosperm cellularization stage at ~96 h (Luo *et al.*, 2005; Matias-Hernandez *et al.*, 2010). Pollinated pistils were stained at 48 and 72 h after pollination (HAP; Figure 2f and g). At 48 HAP, 90.2% of the seeds from wild-type plants showed uniform GUS staining of the developing endosperm, while only 43.1% of *apum24-1*$^{+/-}$ ovules were stained. Fully stained seeds most likely represent wild-type seeds that possess the *apum24*$^{+}$ allele. In the remaining progeny of *apum24-1*$^{+/-}$ plants, staining was observed either at the tip of the micropylar end (Figure 2f, right panel) suggesting that the staining was just initiated at the site of developing zygote (Figure 2g, **), or no staining was observed at all (Figure 2g, *). At 72 HAP, however, there was a striking increase in GUS staining in *apum24-1* seeds. The number of seeds showing full endosperm staining increased to 83.3% and the unstained seeds were reduced to 7.5% (Figure 2g). This was a similar staining pattern to that observed for the wild-type seeds at 48 HAP. Initially, when the siliques were dissected to study the seed setting defect, 19.2% seeds of self-fertilized *apum24-1*$^{+/-}$ siliques were counted as aborted ovules (Table S1). The positive GUS staining by *MINI3:GUS* expression shows that such ovules were indeed fertilized but aborted at very early stages of seed development. Taken together, fertilization occurred normally in *apum24-1* mutant ovules but was delayed, suggesting that female gametophytic effects influence cell division of the zygotic embryo and endosperm, at least in part.

Division of endosperm cells occurs at a slower rate in *apum24*

To further examine post-fertilization development of *apum24-1*$^{+/-}$ pistils, we made use of *AT5G01860:n1GFP* marker line (Wang *et al.*, 2010) that expresses GFP in the dividing endosperm nuclei of the fertilized wild-type embryo sac (Figure 2h), as well as in the nuclei of all four cell types of female gametophyte (i.e. the antipodal, synergid, central and egg cells; Figure S9). In wild-type seeds, post-fertilization expression was observed not only in endosperm nuclei but also in the nuclei of antipodal cells (Figure 2h). Developing wild-type seeds also showed ectopic expression with a frequency of less than 1% (Figure 2h and i). Our study did not reveal a significant difference in ovule development before pollination in wild-type and *apum24-1*$^{+/-}$ plants (Table S7). However, at 24 HAP, whereas wild-type seeds were present at the 16-cell stage, *apum24-1*$^{+/-}$ seeds were at various stages ranging from 2- to 16-cell stages (Figure 2h). Quantitatively, 76.7% of seeds from wild-type plants reached the 16-cell endosperm stage at 24 HAP. In contrast, 36.5% of *apum24-1*$^{+/-}$ endosperms were at the 16-cell stage, and 12 and 23% were at the 2- and 4-cell stages, respectively (Figure 2i). This result demonstrates that the *apum24-1*$^{+/-}$ endosperm was developmentally delayed after fertilization when compared with wild-type endosperm.

Overall, our results indicate that APUM24 is not essential during mega-gametogenesis but rather required for the timely development of embryo and endosperm after fertilization. Hence, the aborted ovules observed in mutant siliques (Figure 2c; Table S1) are indeed fertilized seeds that were aborted at early stages of embryo development, which is also evident as small fluorescent dots in *MINI3:GUS* (Figure 2f).

APUM24 is essential for embryonic development and patterning

Next, to examine which stages of embryos were arrested, we compared the embryos within a single silique that contains both developing wild-type and mutant seeds (Figure 3a). The growth rate of the embryo proper was easily distinguished between two types of seeds. That is, when wild-type embryos were at the mid-globular to cotyledonary stages, the mutants were at single cell to late globular stages and did not develop beyond the globular stage. In addition, aberrant division pattern was also observed in mutant suspensor cells. Whereas wild-type suspensor cells divided transversely to give rise to a single file of cells, some of the mutant suspensor cells not only divided longitudinally but also appeared swollen and enlarged (Figure 3a, white arrowheads). Abnormal cell division was also frequently observed in the hypophysis of mid-globular stage embryos in mutant (red-colored arrowhead). Therefore, *APUM24* is required for normal cell division patterning during early embryogenesis and thus its loss-of-function causes embryos being arrested before the globular stage.

Because the cell division pattern appeared to be abnormal in mutant embryos, we observed the morphology of embryonic cells in more detail (Figure 3c). Although most of the *apum24-1* pro-embryos underwent normal cell division as wild-type embryos (Figures 3b and c), approximately 9.5% of mutant pro-embryos showed transverse or oblique cell division and failed to grow further. Mutant embryos that survived at the pro-embryo stage developed to octant embryos; however, the hypophysis cells of octant stage mutant embryos divided either longitudinally or obliquely at a rate of 37.8%. In wild-type embryos, the hypophysis cell divides asymmetrically to give rise to a lens-shaped upper hypophysis derivative (UHD, the precursor

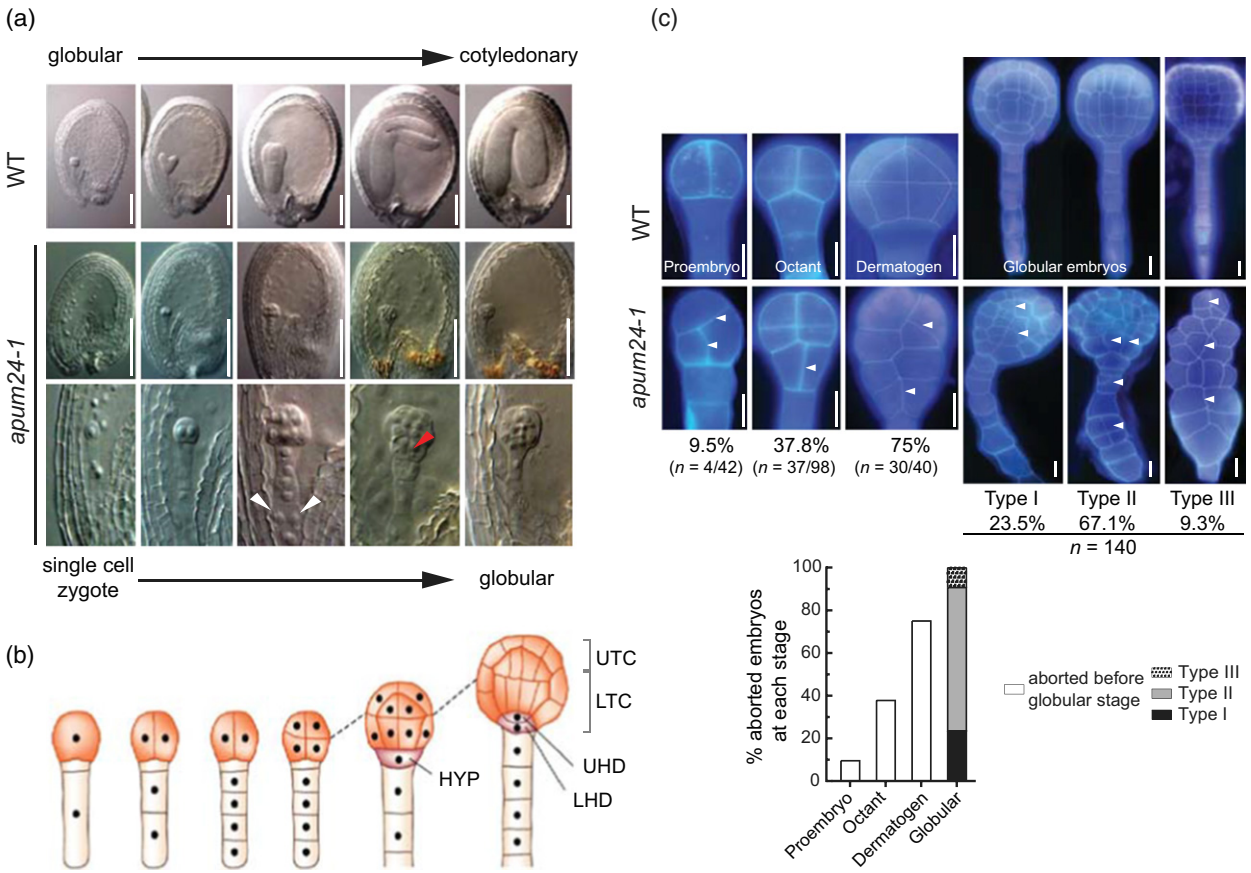

Figure 3. *apum24-1* embryos are aborted before the globular stage.
(a) Comparison of *apum24-1* and wild-type embryos within a single silique from an *apum24-1*$^{+/-}$ plant. Mutant embryos grow slowly and fail to develop beyond the globular stage (middle panel). In the mutant, abnormal suspensor cells displaying a vertical division (white arrowheads) and the hypophysis with a longitudinal division (red-colored arrowhead) are shown in the magnified photos (bottom panel). Scale bars: 100 μm.
(b) Diagram of normal division patterns in wild-type embryo. HYP, hypophysis; UTC, upper tier of cells; LTC, lower tier of cells; UHD, upper hypophysis derivative; LHD, lower hypophysis derivative.
(c) Aberrant cell division patterns appearing at each stage of pre-globular to globular *apum24-1* embryos. Embryos were stained with Calcofluor white to visualize cell wall. Arrowheads indicate the abnormal division planes. The *n* represents the number of embryos showing abnormal divisions per total number of embryos at the corresponding stage. The *apum24-1* embryos that survived and developed to the globular stage were classified into three classes (type I, II and III) depending on cell division pattern. Abortion of *apum24-1* embryos began from the pro-embryo stage and ended at the globular stage (graph). Scale bars: 10 μm. [Colour figure can be viewed at wileyonlinelibrary.com].

of quiescent center) and a basal lower hypophysis derivative (LHD) cell at the transition from the dermatogen to late globular stage (Figure 3b; Mayer *et al.*, 1993; Hardtke and Berleth, 1998). About 75% of the embryos that survived at the octant stage showed perpendicular or oblique divisions thereby producing abnormal dermatogen embryos, while wild-type embryos divided periclinally during the transition from octant to dermatogen stage. At the globular stage, *apum24-1* embryos showed an elongated or spherical shape with irregular arrangement of cells. We divided the *apum24-1* mutant globular embryos into three categories: type I had abnormal and misplaced division planes (23.5%); type II had abnormal globular cells and the enlarged and bloated suspensor cells (67.1%); and type III lacked the globular shape and apical-basal polarity (9.3%; Figure 3c). In type II mutant embryos, the major class of aborted globular embryos, the average cell number and area of suspensor were 1.26-fold more and 2.08-fold wider than those of wild-type suspensor (Table S8). Overall, although *apum24-1* embryos could pass through the early stages of development, they were eventually terminated at the late globular stage, indicating that *APUM24* is essential for proper cell division and pattern formation during embryogenesis.

Auxin distribution and transport are disrupted in *apum24* embryos

Asymmetric auxin localization is important for embryonic patterning as well as other multiple developmental processes (Petrasek and Friml, 2009). Abnormal cell division

patterns in *apum24-1* embryos raised the possibility of impaired auxin homeostasis at the early embryo stage. To examine the auxin distribution and transport in *apum24-1* embryos, we crossed *apum24-1*$^{+/-}$ plants with *DR5*$_{rev}$*:GFP*, *PIN1:PIN1-GFP* and *PIN7:PIN7-GFP* transgenics. In wild-type embryos, the *DR5*$_{rev}$*:GFP* reporter expression was localized in the apical cells of pro-embryo and octant embryos, and then accumulated in the hypophysis at the globular and heart stage embryo (Figure 4a). However, in the *apum24-1* embryos, the GFP signal accumulated in large aggregates inside the suspensor cells of the pro-embryo with weak signal in apical cells, and was distributed uniformly in entire cells of quadrant embryos. In the mutant globular embryos, GFP was not located around the hypophysis, but instead was distributed throughout the entire embryo, in contrast to that observed in wild-type embryos at the globular stage. Our auxin reporter data suggested a defect in the establishment of an apical-basal auxin gradient in *apum24-1* embryos.

During embryogenesis, PIN1-GFP predominantly localizes in the cell membrane of the embryo proper in wild-type embryos (Figure 4b). However, *apum24-1* globular embryos showed unusual PIN1-GFP localization in the subepidermal cells of embryo proper with large intracellular aggregates that are most likely endosomal compartments (Figure 4b). Like PIN1, PIN7 also follows a precise localization pattern (Friml *et al.*, 2003). In wild-type globular embryos after about the 32-cell stage, PIN7-GFP localizes to the basal membrane of suspensor cells thereby enabling basipetal transport of auxin (Figure 4c). However, the *apum24-1* mutant embryos showed a loss of polarity of PIN7-GFP localization as GFP signal was observed throughout the entire plasma membrane of the suspensor cells (Figure 4c), which may result in non-vectorial auxin transport and in turn unpredictable cell division, such as longitudinal cytokinesis. Our results showing an altered localization and polarity of PIN1 and PIN7 in *apum24-1* mutant embryos suggest that *APUM24* is required for proper auxin flow and embryonic pattern formation.

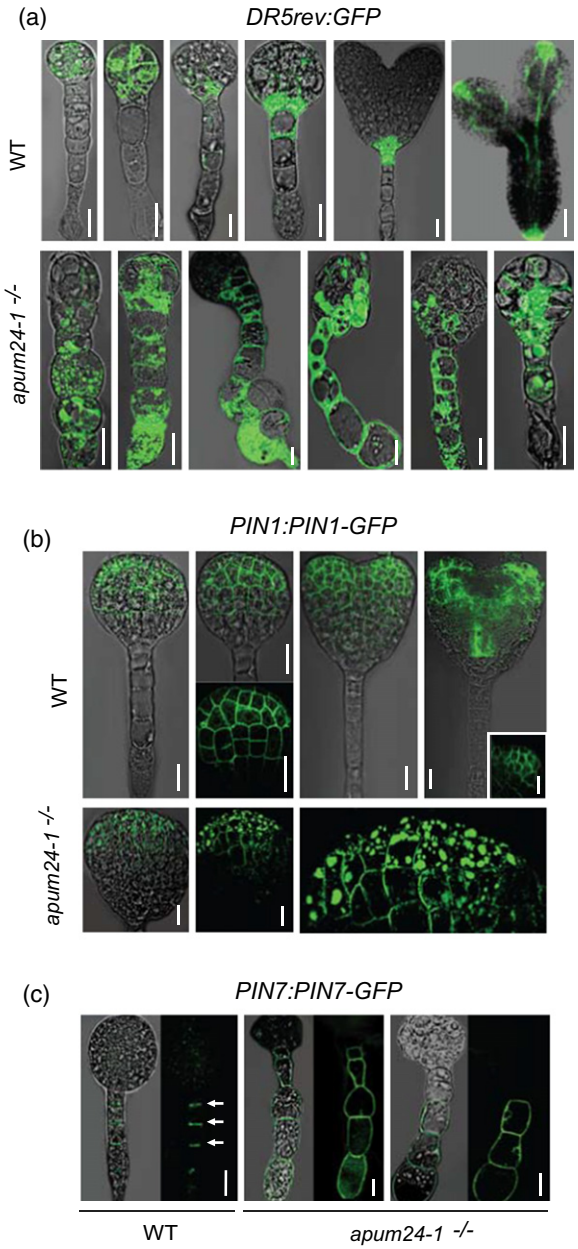

Figure 4. *apum24-1* embryos display a disrupted distribution of auxin and auxin transporters.
(a) Abnormal *DR5*$_{rev}$*:GFP* expression in *apum24-1*$^{-/-}$ embryos.
(b) *PIN1:PIN1-GFP* expression in wild-type and *apum24-1*$^{-/-}$ embryos.
(c) *PIN7:PIN7-GFP* expression in wild-type and *apum24-1*$^{-/-}$ embryos. PIN7-GFP localizes in the basal membrane of each suspensor cell of wild-type globular embryos (arrows), but is equally distributed along the suspensor cell membranes in mutant embryos. Scale bars: 20 μm. [Colour figure can be viewed at wileyonlinelibrary.com].

APUM24 is required for the processing of 27SB and 5.8S rRNA

As APUM24 localizes in the nucleolus and is phylogenetically closely related to yeast Puf6 and nucleolar APUM23, it might be involved in rRNA processing (Abbasi *et al.*, 2010; Qiu *et al.*, 2014). Ribosomal RNA (rRNA) processing is a complicated and highly coordinated event through which 35S pre-rRNA is processed using multiple endonucleases and exonucleases resulting in the production of mature 18S, 5.8S and 25S rRNAs (Lange *et al.*, 2011; Hang *et al.*, 2014; Weis *et al.*, 2015a). In Arabidopsis, a few rRNA cleavage sites are known, which include the P, P1 and P′ sites in 5′ ETS, the A2 and A3 sites in ITS1, the C2 site in the ITS2, and the B0 site in 3′ ETS (Weis *et al.*, 2015a; Figure 5a).

To examine rRNA processing in the *apum24* mutant, we performed RNA gel blot analysis using total and poly(A) RNA isolated from callus derived from rescued homozygous *apum24* globular embryos (Figures 5 and S10). Based on known cleavage sites of Arabidopsis (Weis *et al.*,

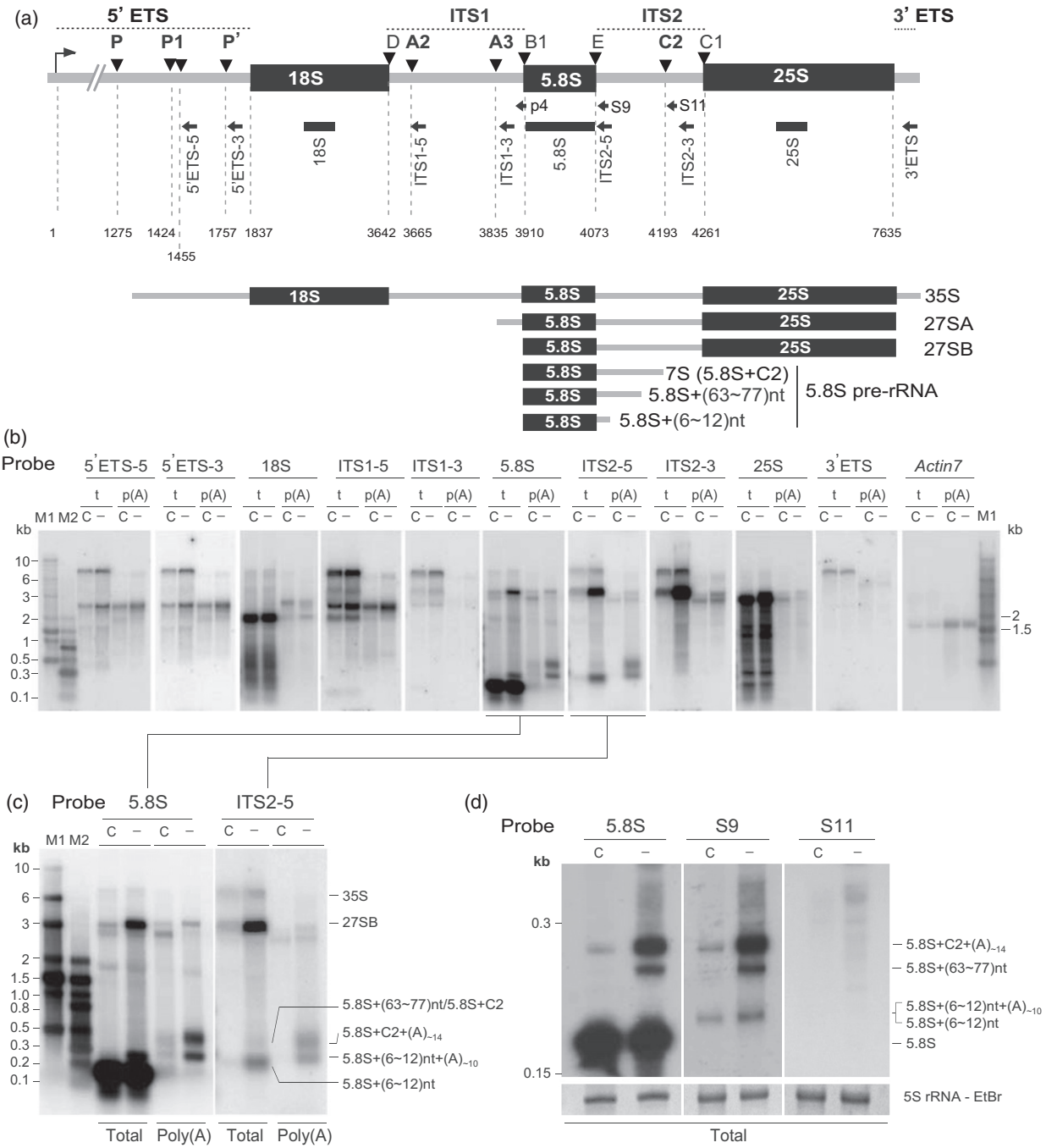

Figure 5. Accumulation of 3′-extended 5.8S rRNA and 27SB pre-rRNA in *apum24-1*$^{-/-}$ embryo-derived callus.
(a) Diagram of the Arabidopsis rDNA gene and intermediate transcripts. Processing sites are indicated by arrowheads. The regions used for oligonucleotide and cDNA probes are indicated with horizontal arrows and black lines, respectively. The nucleotide positions are indicated with reference to the +1 transcription start (bent arrow).
(b) rRNA gel blots for total and poly(A) RNAs isolated from the calli derived from wild-type and *apum24*$^{-/-}$ globular embryos. *Actin7* was used as a loading control RNA. t, total RNA; p(A), poly(A) RNA; C, wild-type Col-3 control; –, *apum24-1*$^{-/-}$; M1 and M2, RNA size markers.
(c) Enlarged images of 5.8S and ITS2-5 rRNA gel blots in (b) Transcript types accumulated in *apum24*$^{-/-}$ are denoted on the right.
(d) Northern analysis of 5.8S rRNA precursors with 5.8S, S9 and S11 probes using total RNA from wild-type Col-3 and *apum24-1*$^{-/-}$ callus on 6% denaturing polyacrylamide gels. Note the three major types of 3′-extended 5.8S pre-rRNAs accumulated in the mutant callus. The deciphered identities of 5.8S extended forms from circular reverse-transcriptase-polymerase chain reaction (cRT-PCR) assays (Figure S12) are denoted on the right.

2015a) and yeast (Henras *et al.*, 2015), site-specific oligonucleotide and cDNA probes were prepared. RNA gel blots revealed no significant difference in the band pattern of total and poly(A) RNA from wild-type and mutant cells when hybridized with the 5′ ETS-5, 5′ ETS-3, 18S, ITS1-5, ITS1-3, 25S and 3′ ETS probes with slightly higher accumulation of 35S primary transcripts (Figure 5b). However, clear rRNA processing defects were observed in blots probed with 5.8S, ITS2-5 and ITS2-3 sequences (Figure 5b and c).

The total RNA blot for *apum24-1* showed an accumulation of 27S pre-rRNA hybridized with 5.8S, ITS2-5 or ITS2-3 probes, while the same blot for wild-type displayed a weak signal. This 27S pre-rRNA was present at a very low level in poly(A) RNA from wild-type cells, but accumulated in mutant cells. The identity of 27S pre-rRNA was further investigated in total RNA gel blots with the oligoprobes S9 and p4 that were previously used to detect 27SA and 27SB precursors (Lange *et al.*, 2011; Hang *et al.*, 2014; Weis *et al.*, 2015a,b; Figure S11a and b). Probe S9, positioned at the 5′-end of ITS2, detected three bands while probe p4, situated at the 3′-end of ITS1, recognized a single band that is longer than 6 kb and thus corresponds to 35S pre-rRNA (Figure S11). In the same context, the strong band that was detected by probes 5.8S and ITS2-5 is 27SB pre-rRNA (Figure 5c). Further, we map the extremities of the 5′- and 3′-ends of 27SB in *apum24-1* mutant using circular cRT-PCR and sequencing (Figure S11c). A majority of the transcripts (47.9%, $n = 48$) were terminally uridylated immediately after the 3′-end of 25S mature RNA sequence in *apum24-1*, while some had cytosine at the 3′-end (18.8%) or poly(A) tail with uridine insertion(s) (10.4%). Therefore, most of the accumulated 27SB transcripts are very likely pre-rRNA byproducts with untemplated tails that are eventually destined to decay pathway.

Besides 27SB pre-rRNA, longer forms of RNAs over 5.8S rRNA were highly accumulated in the mutant (Figure 5b and c; probes 5.8S and ITS2-5). For better resolution, total RNA was fractionated on polyacrylamide gel and blot was probed with 5.8S, S9 and S11 (Figure 5d). Probe S9 detected three distinct bands that were not recognized by probe S11, and thus very likely the transcripts cleaved before C2 site (Figure 5d). Each of these three bands contained heterogeneous 3′-termini as evidenced by cRT-PCR and nucleotide sequence; 5.8S + (6–12)nt, 5.8S + (63–77)nt and 5.8S + C2 (Figure S12b). Among the analyzed three extended forms, the 5.8S + (63–77)nt had no untemplated 3′-terminus or contained 1–3 uridine and/or adenine nucleotide(s), and were not seen in poly(A) blots (Figure 5c). Hence, only polyadenylated 5.8S + (6–12)nt and 5.8S + C2 were detected in poly(A) blots. In addition to (poly)adenylation, the 5.8S extended transcripts were frequently uridylated or rarely contained C and G insertions in tails. Taken together, *apum24* accumulated three dominant categories of 5.8S extended transcripts and 27SB byproducts with varying 3′-terminal modifications.

Recombinant 6xHis-APUM24 binds to *in vitro* transcribed 5.8S and ITS2 RNAs

Yeast homolog of APUM24, Puf6, was found to bind DNA or RNA with no apparent specificity despite its disruption resulting in the specific accumulation of 7S pre-rRNA (Qiu *et al.*, 2014). Puf proteins have long been known to bind RNA and, because APUM24 may target 7S pre-rRNA (5.8S + C2) as one of the binding substrates, we performed an RNA-protein EMSA to test whether APUM24 is capable of binding to the 5.8S and ITS2 sequence (Figure 6a). Band shift analysis using the truncated 71 nt 5.8S rRNA and 6xHis-APUM24 showed broad bands of shifted RNA in common for *in vitro* transcribed 5.8S-1 and 5.8S-2 rRNA (Figure 6b). No shifted band was seen when either rRNA or 6xHis-APUM24 were absent or when Puf domains were deleted. Similarly, broad shifted bands were also observed for the full-length ITS2 sequence, and their migration was dependent on protein dosage (Figure 6c). The broad bands and protein dosage-dependent migration suggest that RNA-APUM24 binding continued until the entire sequence was saturated with APUM24, independent of the RNA sequence. To determine if a smaller ITS2 sequence has differential binding activity with APUM24, we divided the ITS2 into three segments and analyzed the binding of 68–70-nt-long transcripts with 6xHis-APUM24 and 6xHis-APUM24△Puf (Figure 6d). Shifted bands were obtained for ITS2-1, ITS2-2 and ITS2-3 in the presence of 6xHis-APUM24 but not in the absence of protein. Comparison of the ITS2-1, ITS2-2 and ITS2-3 sequences did not show significant homology (Figure S13), although the possibility of structural conservation among them could not be ruled out. Overall, our EMSA study on the 6xHis-APUM24 expressed in bacteria and the *in vitro* transcribed truncated 5.8S and ITS2 pre-rRNA sequences suggests that APUM24 may bind to RNA independent of RNA sequence *in planta*.

Next, to determine the role of Puf domains on RNA binding and nucleolar localization of APUM24, we transiently expressed APUM24ΔPuf-GFP, which has no Puf domains but contains N-terminal nucleolar localizing signals (NoLS), in tobacco leaf cells (Figure S14). APUM24-GFP and APUM24ΔPuf-GFP showed nucleolar localization pattern in common, suggesting that Puf domains do not contribute to the subnuclear distribution of APUM24.

DISCUSSION

The APUM24 clade of Puf proteins is found in all eukaryotes (Abbasi *et al.*, 2010; Tam *et al.*, 2010; Qiu *et al.*, 2014). Despite their similar primary structure, APUM24 homologs have slightly different intracellular localization patterns. APUM24-GFP predominantly localizes in the nucleolus, whereas human Puf-A is found throughout the entire

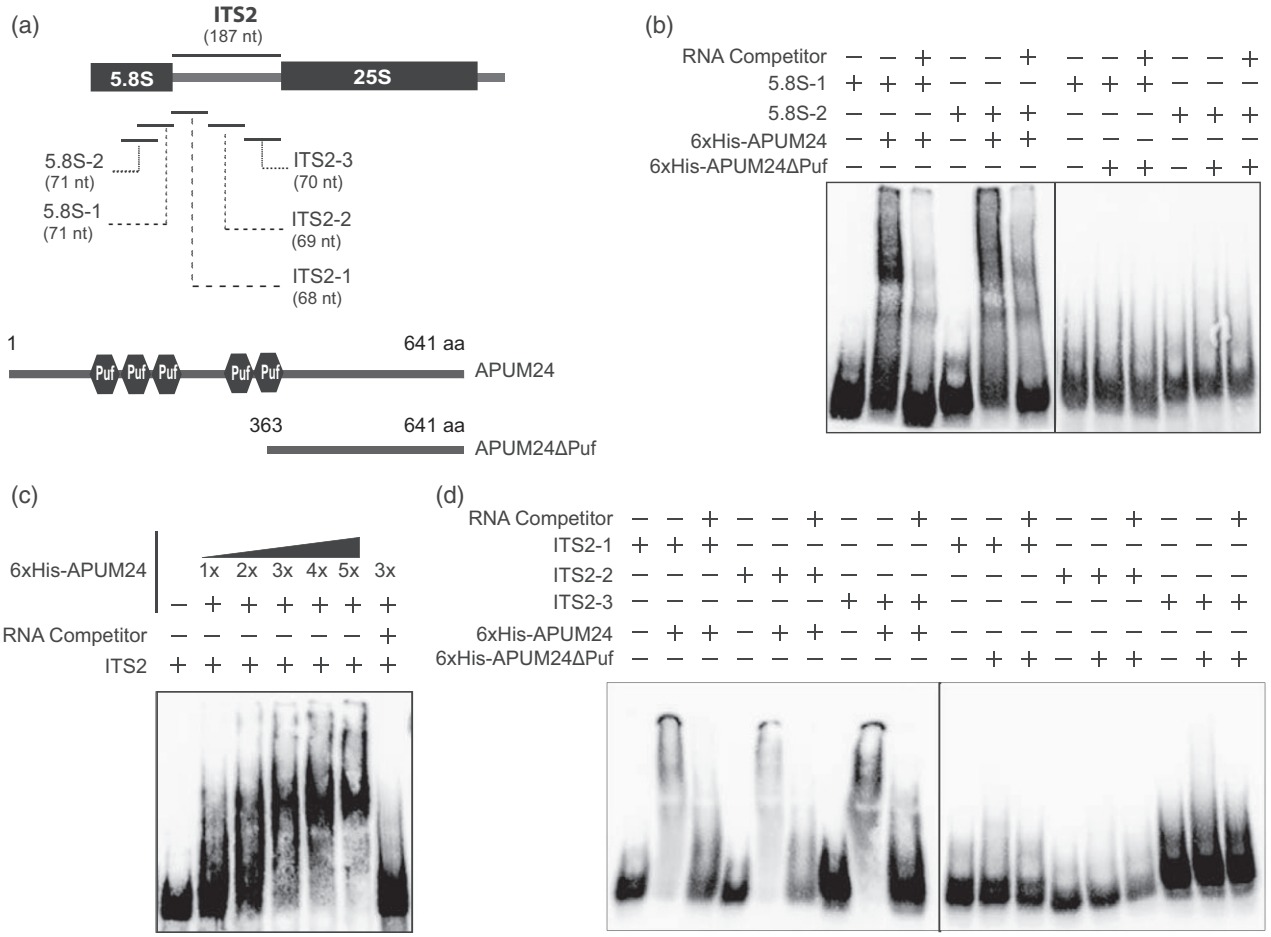

Figure 6. 6xHis-APUM24 interacts with *in vitro* transcribed 5.8S and ITS2 segments.
(a) Diagrams displaying rRNA fragments and the full-length and truncated APUM24 proteins used for RNA-protein binding assay. *In vitro* synthesized rRNA was 3′ end-labeled with biotin.
(b) Binding of 6xHis-APUM24 and 6xHis-APUM24ΔPuf with 5.8S rRNA segments. 6xHis-APUM24, but not 6xHis-APUM24ΔPuf, binds to the 3′ half of the 5.8S rRNA sequence.
(c) Binding of 6xHis-APUM24 to the full-length ITS2 transcript. Increasing 6xHisAPUM24 dosage shows a more shifted pattern. The addition of 45-fold cold ITS2 competitor abolished binding.
(d) Electrophoretic mobility shift assay (EMSA) of 6xHis-APUM24 and 6xHis-APUM24ΔPuf with partial ITS2 sequences. All three fragments (ITS2-1, ITS2-2 and ITS2-3) are not bound by 6xHis-APUM24ΔPuf.

nucleolus and nucleoplasmic speckles (Chang *et al.*, 2011), and the budding yeast ortholog (Puf6) shuttles between the nucleus and cytoplasm (Gu *et al.*, 2004; Deng *et al.*, 2008). Puf6 is involved in rRNA processing (Qiu *et al.*, 2014) and in translation repression-coupled *Ash1* mRNA transport (Gu *et al.*, 2004). Human Puf-A regulates cell viability to genotoxic stress (Chang *et al.*, 2011), while Zebrafish Puf-A functions during embryo development (Kuo *et al.*, 2009). These reports suggest that APUM24 homologs have diverse biological functions depending on their subcellular localization.

APUM24 was expressed in all tissues examined, however, at lower levels in older tissues and cells as demonstrated by the expression of *APUM24:GUS* and *APUM24:APUM24-GFP* plants. The 1086-bp-long promoter used for the expression analysis appears to be sufficient because the intergenic region between the 5′-end of *APUM24* coding sequence and the 3′-end of upstream gene spans only 560 bp. Similar to *APUM23* (Abbasi *et al.*, 2010), *APUM24* expression was increased by sugar supplementation, suggesting its role for orchestrating cell division and growth.

Several Arabidopsis mutants defective in nucleolar functions have been reported to be embryonic lethal due to delayed or impaired ribosome biosynthesis. These mutants have defects in the genes controlling cell division and influencing the division planes during embryogenesis, such as *Domino1* (Lahmy *et al.*, 2004), *SWA1* (Shi *et al.*, 2005), *SWA2* (Li *et al.*, 2009), *SWA3* (Liu *et al.*, 2010), *TOZ* (Griffith *et al.*, 2007), *YAO* (Li *et al.*, 2010), *AtRH36* (Huang *et al.*, 2010) and *NOF1* (Harscoet *et al.*, 2010). Among the

mutants of these reported genes, the *swa1* and *atrh36* mutants are defective in female gametophyte, while the *nof* mutant is affected in female gametogenesis and embryo development. The mutants of all the three genes accumulated 18S rRNA intermediates and displayed abnormal cell cycle. Our results showing that APUM24 affects cell cycle progression and division planes during embryogenesis serve as another example of a nucleolar protein involved in cell division. Although *APUM24* is expressed in all tissues undergoing active proliferation, its mutation showed major developmental defects in embryo and endosperm development. In the same context, the *apum24-2* leaky mutant set shrunken seeds but showed no visible phenotype in the vegetative stage. This phenomenon might not be due to redundancy with other Puf proteins such as APUM23, as only two Puf proteins are known to localize in the nucleolus and their mutants show distinct rRNA processing defects. Actively dividing cells require a rapid supply of mature rRNAs, which is likely achieved in part by APUM24. When a fertilized zygote cell develops into heart stage embryos, it undergoes striking changes in fate determination, such as the differentiation of meristem and vascular tissue that require mature rRNAs to cope with active translation.

The *apum24* mutant embryo was defective in pattern formation from the very early pro-embryo stage to the globular stage (Figure 3). Mutant embryos expressed the *DR5rev:GFP* auxin reporter at high levels in both the embryo proper and suspensor, which was in contrast to the accumulation and distribution pattern from WT embryos. Auxin is involved in highly ordered cell divisions that establish proper embryonic patterning (Möller and Weijers, 2009; Petrasek and Friml, 2009; ten Hove *et al.*, 2015), and its mislocalization is likely responsible for the aberrant cell division in *apum24* mutant embryos. The protoderm and inner cells of mutant embryos showed atypical divisions throughout the octant to globular stages, and thus future differentiation of epidermal, vascular and ground cells was not established. Moreover, a lack of asymmetric cell division in the embryo proper probably results in the failure of apical-basal fate separation. It is likely that a high auxin concentration in the suspensor of the mutant embryo may have resulted from mislocalized auxin transporters (Figure 5). We conclude that abnormal subcellular localization of auxin transporters in the *apum24* mutant embryo caused irregular cell division and organ differentiation.

Our rRNA processing data using *apum24* callus showed the accumulation of polyadenylated 5.8S + C2 in 7S pre-rRNA position on the blot. Processing defect of 7S pre-rRNA indicates a lack of exosome function (Mitchell *et al.*, 1997). In yeast, the mutants that are defective in Rrp4, Rrp40, Rrp41, Rrp42, Rrp43, Rrp44, Rrp45, Csl4, Dob1p/Mtr4p or Rrp6 protein also accumulated 7S pre-rRNA (Mitchell *et al.*, 1997; de la Cruz *et al.*, 1998; Kiss and Andrulis, 2011). Similarly in Arabidopsis, exosome subunit mutants, *csl4*, *rrp4*, *rrp41* and *rrp6l2* accumulated 7S pre-rRNA (Chekanova *et al.*, 2007; Lange *et al.*, 2008). Further, Arabidopsis *mtr4* (Lange *et al.*, 2011; Sikorski *et al.*, 2015), *rrp4* (Hématy *et al.*, 2016), *rrp41* (Chekanova *et al.*, 2000) and *rrp44a* (Kumakura *et al.*, 2013) mutants displayed an accumulation of other 5.8S intermediates, similar to *apum24.* Our cRT-PCR analysis showed a heterogeneous population of transcripts corresponding to varying lengths of 5.8S + (6–12)nt and 5.8S + (63–77)nt. In addition to 3′-extended 5.8S pre-rRNA, the *apum24* mutant accumulated 27SB pre-rRNA with or without untemplated 3′-extensions. The accumulation of 27SB pre-rRNA was most likely due to its delayed processing and/or decay defect, as a similar accumulation of 27S pre-rRNA was observed previously in a *RRP43* mutant and *Dob1*/*Mtr4* mutant in which rRNA processing is severely delayed (de la Cruz *et al.*, 1998; Zanchin and Goldfarb, 1999). The 3′-uridylation is a widespread phenomenon in the RNAs undergoing degradation (Scheer *et al.*, 2016). In the Arabidopsis *rrp6l2* mutant defective in 18S rRNA processing, the accumulating 18S-A2 rRNA and 5.8S precursors are uridylated at the 3′-ends (Sikorski *et al.*, 2015), similar to 27SB and 5.8S intermediates in *apum24* mutant. Hence, the 3′ addition of uridine to aberrant rRNAs might be very common prior to degradation. In our current study, the histidine-tagged APUM24 expressed in *Escherichia coli* bound to *in vitro* transcribed 5.8S and ITS2 RNA sequences. However, it remains to be solved whether APUM24 binds to 3′-extended 5.8S pre-rRNA *in planta*. Native APUM24 and rRNA may undergo site-specific modification, but also have their intrinsic folding structures. For instance, the Arabidopsis 5.8S rRNA was predicted to have $^{m}G_{79}$ that are contained in the EMSA probe 5.8S-2, although other probe sequences used in our study are not reportedly modified (Brown *et al.*, 2003; Piekna-Przybylska *et al.*, 2008).

In summary, APUM24 functions in rRNA processing through its RNA binding activity and is essential for early embryogenesis. Defects in APUM24 resulted in embryonic lethality, similar to the mutants of other essential ribosome biogenesis factors. As protein synthesis is active during early embryonic development, dysfunction of the protein synthetic machinery would have lethal outcomes prior to the development of complex tissues and organs.

EXPERIMENTAL PROCEDURES

Plant materials, growth conditions and mutant screening

The following seed stocks were obtained from the Arabidopsis Biological Resource Center (ABRC): Col-3 (CS908), *apum24-1* (SAIL_75_E07), *apum24-2* (SALK_033623), *apum24-3* (GABI_461E08), *DR5rev:GFP* (CS9361) and *qrt1-4* (SALK_024104C). *Arabidopsis thaliana* wild-type and mutants were grown on soil under 16-h light (120 μmol photons m^{-2} sec^{-1})/8-dark photoperiod at 22°C. For sugar treatments, wild-type seeds were surface-sterilized with 70%

ethanol, stratified at 4°C for 3 days, and germinated on MS medium. The mutant alleles *apum24-1*, *apum24-2* and *apum24-3* were genotyped by PCR using primers specific for the T-DNA inserts (LB3, LBb1.3 and LB, respectively) and *APUM24* gene-specific primers, APUM24-1F, APUM24-1R, APUM24-2F, APUM24-2R, APUM24-3F and APUM24-3R (see Table S9 for primers). For selection, 50 μg ml^{-1} Basta® (DL-Phosphinothricin, Duchefa, https://www.duchefa-biochemie.com/), 50 μg ml^{-1} kanamycin or 50 μg ml^{-1} sulfadiazine (Sigma-Aldrich, http://www.sigmaaldrich.com/) was added to the MS medium.

Complementation, plasmid construction and Arabidopsis transformation

For complementation assay, a 6065-bp genomic DNA fragment of TAC clone, K20I9, from ABRC was digested with *Nco*I. This genomic fragment includes the 1.4-kb upstream sequence of the translational start and the 0.5-kb downstream of stop codon. The DNA fragment was subcloned in pET30a, then removed using *Kpn*I and *Bam*HI, and cloned into pCAMBIA1301 to produce CAMBIA1301-APUM24-6K. This construct was transformed into *apum24-1*$^{+/-}$ plants by floral-dipping using the *Agrobacterium tumefaciens* GV3101. T1 plants were selected on MS medium containing both Basta® and Hygromycin (Duchefa), and their seeds were plated on MS medium containing both the chemicals. The segregation ratio was counted in the T2 generation.

The constructs for N-terminal 6xHis-tagged APUM24 (6xHis-APUM24) and the 6xHis-tagged APUM24 without N-terminal 362 amino acids (6xHis-APUM24ΔPuf) were generated by RT-PCR (see Table S9 for primers). PCR-amplified products were digested and cloned into pET30c. Plasmid construction procedures for the *35S:GFP-APUM24*, *35S:APUM24-GFP* and *APUM24:APUM24-GFP* that are used for the subcellular localization and tissue expression studies are provided in Methods S2.

Northern blotting and cRT-PCR

For RNA gel blot analysis, total RNA was isolated using TRIzol® reagent (Thermo Fisher) from the calli induced from Col-3 and *apum24-1* globular embryos (see Methods S1 for callus induction). Poly(A) RNA was isolated from calli using the Dynabead® mRNA DIRECT Kit (Thermo Fisher). Five micrograms of total RNA and 0.5 μg of poly(A) RNA were separated on 1.2% agarose gels containing 5% formaldehyde, or on acrylamide gels containing 7 M urea, 6% polyacrylamide and TBE (90 mM Tris, 90 mM boric acid and 2 mM EDTA, pH 8.2), and transferred to Hybond-NX membrane (GE Healthcare, http://www.gelifesciences.com/). Random-labeled cDNA probes were used for mature 18S, 5.8S and 25S rRNA, while end-labeled oligonucleotides were used to detect the external transcribed sequence (ETS) and internal transcribed sequence (ITS). DNA templates for 18S, 5.8S, 25S and *Actin7* were obtained by PCR, cloned into pGEM-T Easy (Promega) and confirmed by sequencing. An *Eco*RI fragment was labeled with [α-^{32}P]-dCTP (3000 Ci mmol^{-1}; PerkinElmer, http://www.perkinelmer.com/). For the labeling of oligonucleotides, 50 pmol of oligonucleotide was incubated with 50 pmol of [γ-^{32}P]-ATP (3000 Ci mmol^{-1}) in 50 μl of reaction mixture containing T4 polynucleotide kinase (NEB, https://www.neb.com/). Hybridization and data acquisition were done as described previously (Abbasi *et al.*, 2010). cRT-PCR procedures are described in Methods S3.

RNA electrophoretic mobility shift assay (EMSA)

The 6xHis-APUM24 and 6xHis-APUM24ΔPuf proteins were expressed for EMSA in *E. coli* BL2 (DE3)-RIL by 0.5 mM IPTG for 6 h at 28°C and purified using Ni-NTA Agarose (Thermo Fisher). The eluted protein sample was loaded onto a Sephadex® G-25 column (GE Healthcare), desalted using Exchange/Storage buffer (100 mM HEPES, pH 7.4, 200 mM KCl, 0.1 mM EDTA, 1 mM DTT, 10% glycerol), and concentrated using 10 kDa cut-off spin concentrator (Vivaproducts, http://www.vivaproducts.com/).

Full-length ITS2 and 5.8S rDNA regions were cloned into pGEM-T Easy and verified by sequencing. DNA fragments were PCR-amplified using primer pairs for ITS2, ITS2-1, ITS2-2, ITS2-3, 5.8S-1 and 5.8S-2, of which each upstream primer contains T7 promoter sequence. An *in vitro* transcription reaction was performed using DuraScribe® T7 Transcription kit (Epicentre, http://www.epibio.com/), and RNA was purified using a NucAway™ Spin column (Thermo Fisher). Labeling was performed with 50 pmol of RNA using RNA 3′ End Biotinylation kit (Thermo Fisher). Labeled RNA was then incubated for 5 min with 6xHis-APUM24 and 6xHis-APUM24ΔPuf in binding buffer [100 mM HEPES, pH 7.2, 160 mM KCl, 0.5 mM EDTA, 50% glycerol, 350 ng μl^{-1} BSA, 40 ng μl^{-1} poly (dI-dC), 12.5 mM DTT] and resolved on 4% Native PAGE. RNA was transferred onto a membrane, and developed with Chemiluminescent Nucleic Acid Detection Module (Thermo Fischer).

Microscopic techniques

Procedures for histochemical fluorescence staining and confocal laser-scanning microscopy are described in Methods S4.

ACCESSION NUMBERS

Sequence data for the genes described in this article can be found in the Arabidopsis Genome Initiative under the following accession numbers: *Act7* (AT5G09810), *APUM24* (AT3G16810), *MINI3* (AT1G55600), *PIN1* (AT1G73590), *PIN7* (AT1G23080) and *Tub2* (AT5G62690).

ACKNOWLEDGEMENTS

The authors thank Abed Chaudhury (CSIRO, Australia) for *MINI3:GUS* line, and Hyung-Taeg Cho (SNU) for the *PIN1:PIN1-GFP* and *PIN7:PIN7-GFP* seeds. The gametophytic marker lines were obtained from Gary Drews (University of Utah), and the *H3.3:H3.3-mRFP1* line was from Frederic Berger (Gregor Mendel Institute). The seeds for *AT5G01860:n1GFP* were a gift from Ramin Yadegari (University of Arizona). This work was supported by grants from the National Research Foundation (NRF-2014R1A2A1A11051569) and from the Next-Generation BioGreen21 Program, Rural Development Administration (No. PJ011120), Korea, to SBC.

CONFLICT OF INTEREST

The authors declare no conflict of interest.

SUPPORTING INFORMATION

Additional Supporting Information may be found in the online version of this article.

Figure S1. Phylogenetic tree of Puf proteins homologous to APUM24.
Figure S2. Nucleolar localization of APUM24.
Figure S3. GUS expression in *APUM24:GUS* plants.
Figure S4. The *apum24-1* mutant pollen is viable.
Figure S5. DAPI staining of *apum24-1*$^{+/-}$ *qrt1-4*$^{-/-}$ pollens.
Figure S6. *APUM24* mutation does not affect the differentiation of vegetative and sperm cell nuclei.
Figure S7. Ovule identity cell development is normal in *apum24-1* mutant.

Figure S8. The *apum24-1* ovules are competent to attract pollen tubes.
Figure S9. *At5g01860:n1GFP* expression during mega-gametogenesis and early embryogenesis.
Figure S10. Callus derived from *apum24-1*$^{-/-}$ embryos.
Figure S11. Accumulation of 3′-extended 27SB pre-rRNA in *apum24* mutant.
Figure S12. Identification of 3′-extended 5.8S pre-rRNAs accumulated in *apum24* mutant.
Figure S13. Substrate RNAs used for RNA-protein EMSA.
Figure S14. Subcellular localization of GFP-tagged full-length and truncated APUM24 proteins in tobacco leaf cells.
Table S1. Seed setting frequency in mature siliques of Col-3 and *apum24* mutants.
Table S2. Segregation ratios of seeds from *apum24-1*$^{+/-}$, *apum24-3*$^{+/-}$ and complemented *apum24-1*$^{+/-}$ alleles on selection medium.
Table S3. Segregation and transmission efficiency of the *apum24-1* mutant allele.
Table S4. Quantitative data generated by DAPI staining of pollen nuclei in *qrt1-4* and *apum24-1*$^{+/-}$ mutants.
Table S5. Quantitative analysis of sperm cells and vegetative nuclei expressing RFP in *apum24-1* mutants, crossed to the marker lines at the anthesis stage.
Table S6. Description of female gametophytic markers used in this study.
Table S7. Synchrony of female gametophyte development in wild-type Col-3 and *apum24-1*$^{+/-}$ plants.
Table S8. Cell number and size of mid-globular stage suspensor in type II embryos.
Table S9. List of primers used in this study.
Methods S1. Callus induction from globular embryos.
Methods S2. Plasmid construction for the subcellular localization and tissue expression analyses.
Methods S3. cRT-PCR.
Methods S4. Microscopy.

REFERENCES

Abbasi, N., Kim, H.B., Park, N.-I., Kim, Y.-K., Park, Y.-I. and Choi, S.-B. (2010) APUM23, a nucleolar Puf domain protein, is involved in pre-ribosomal RNA processing and normal growth patterning in Arabidopsis. *Plant J.* **64**, 960–976.

Bailey-Serres, J., Sorenson, R. and Juntawong, P. (2009) Getting the message across: cytoplasmic ribonucleoprotein complexes. *Trends Plant Sci.* **14**, 443–453.

Barkan, A. and Small, I. (2014) Pentatricopeptide repeat proteins in plants. *Annu. Rev. Plant Biol.* **65**, 415–442.

Belostotsky, D.A. and Sieburth, L.E. (2009) Kill the messenger: mRNA decay and plant development. *Curr. Opin. Plant Biol.* **12**, 96–102.

Brown, J.W., Echeverria, M., Qu, L.H., Lowe, T.M., Bachellerie, J.P., Huttenhofer, A., Kastenmayer, J.P., Green, P.J., Shaw, P. and Marshall, D.F. (2003) Plant snoRNA database. *Nucleic Acids Res.* **31**, 432–435.

Campbell, Z.T., Valley, C.T. and Wickens, M. (2014) A protein-RNA specificity code enables targeted activation of an endogenous human transcript. *Nat. Struct. Mol. Biol.* **21**, 732–738.

Chang, H.Y., Fan, C.C., Chu, P.C., Hong, B.E., Lee, H.J. and Chang, M.S. (2011) hPuf-A/KIAA0020 modulates PARP-1 cleavage upon genotoxic stress. *Cancer Res.* **71**, 1126–1134.

Chekanova, J.A., Shaw, R.J., Wills, M.A. and Belostotsky, D.A. (2000) Poly (A) tail-dependent exonuclease AtRrp41p from *Arabidopsis thaliana* rescues 5.8 S rRNA processing and mRNA decay defects of the yeast *ski6* mutant and is found in an exosome-sized complex in plant and yeast cells. *J. Biol. Chem.* **275**, 33158–33166.

Chekanova, J.A., Gregory, B.D., Reverdatto, S.V. *et al.* (2007) Genome-wide high-resolution mapping of exosome substrates reveals hidden features in the Arabidopsis transcriptome. *Cell*, **131**, 1340–1353.

Cheng, S., Gutmann, B., Zhong, X. *et al.* (2016) Redefining the structural motifs that determine RNA binding and RNA editing by pentatricopeptide repeat proteins in land plants. *Plant J.* **85**, 532–547.

de la Cruz, J., Kressler, D., Tollervey, D. and Linder, P. (1998) Dob1p (Mtr4p) is a putative ATP-dependent RNA helicase required for the 3′ end formation of 5.8S rRNA in *Saccharomyces cerevisiae*. *EMBO J.* **17**, 1128–1140.

Deng, Y., Singer, R.H. and Gu, W. (2008) Translation of *ASH1* mRNA is repressed by Puf6p-Fun12p/eIF5B interaction and released by CK2 phosphorylation. *Genes Dev.* **22**, 1037–1050.

Dong, S., Wang, Y., Cassidy-Amstutz, C., Lu, G., Bigler, R., Jezyk, M.R., Li, C., Hall, T.M. and Wang, Z. (2011) Specific and modular binding code for cytosine recognition in Pumilio/FBF (PUF) RNA-binding domains. *J. Biol. Chem.* **286**, 26732–26742.

Filipovska, A., Razif, M.F., Nygard, K.K. and Rackham, O. (2011) A universal code for RNA recognition by PUF proteins. *Nat. Chem. Biol.* **7**, 425–427.

Francischini, C.W. and Quaggio, R.B. (2009) Molecular characterization of *Arabidopsis thaliana* PUF proteins – binding specificity and target candidates. *FEBS J.* **276**, 5456–5470.

Friml, J., Vieten, A., Sauer, M., Weijers, D., Schwarz, H., Hamann, T., Offringa, R. and Jürgens, G. (2003) Efflux-dependent auxin gradients establish the apical-basal axis of Arabidopsis. *Nature*, **426**, 147–153.

Gennarino, V.A., Singh, R.K., White, J.J. *et al.* (2015) *Pumilio1* haploinsufficiency leads to SCA1-like neurodegeneration by increasing wild-type Ataxin1 levels. *Cell*, **160**, 1087–1098.

Gerber, A.P., Herschlag, D. and Brown, P.O. (2004) Extensive association of functionally and cytotopically related mRNAs with Puf family RNA-binding proteins in yeast. *PLoS Biol.* **2**, E79.

Griffith, M.E., Mayer, U.C.A., Ngo, Q.A., Surendrarao, A., McClinton, R., Jürgens, G. and Sundaresan, V. (2007) The *TORMOZ* gene encodes a nucleolar protein required for regulated division planes and embryo development in *Arabidopsis*. *Plant Cell*, **19**, 2246–2263.

Gu, W., Deng, Y., Zenklusen, D. and Singer, R.H. (2004) A new yeast PUF family protein, Puf6p, represses *ASH1* mRNA translation and is required for its localization. *Genes Dev.* **18**, 1452–1465.

Hang, R., Liu, C., Ahmad, A., Zhang, Y., Lu, F. and Cao, X. (2014) *Arabidopsis* protein arginine methyltransferase 3 is required for ribosome biogenesis by affecting precursor ribosomal RNA processing. *Proc. Natl Acad. Sci. USA* **111**, 16190–16195.

Hardtke, C.S. and Berleth, T. (1998) The *Arabidopsis* gene *MONOPTEROS* encodes a transcription factor mediating embryo axis formation and vascular development. *EMBO J.* **17**, 1405–1411.

Harscoet, E., Dubreucq, B., Palauqui, J.C. and Lepiniec, L. (2010) *NOF1* encodes an Arabidopsis protein involved in the control of rRNA expression. *PLoS ONE*, **5**, e12829.

Hématy, K., Bellec, Y., Podicheti, R. *et al.* (2016) The zinc-finger protein SOP1 is required for a subset of the nuclear exosome functions in Arabidopsis. *PLoS Genet.* **12**, e1005817.

Henras, A.K., Plisson-Chastang, C., O'Donohue, M.F., Chakraborty, A. and Gleizes, P.E. (2015) An overview of pre-ribosomal RNA processing in eukaryotes. *Wiley Interdiscip. Rev. RNA*, **6**, 225–242.

ten Hove, C.A., Lu, K.J. and Weijers, D. (2015) Building a plant: cell fate specification in the early *Arabidopsis* embryo. *Development*, **142**, 420–430.

Huang, C.K., Huang, L.F., Huang, J.J., Wu, S.J., Yeh, C.H. and Lu, C.A. (2010) A DEAD-box protein, AtRH36, is essential for female gametophyte development and is involved in rRNA biogenesis in Arabidopsis. *Plant Cell Physiol.* **51**, 694–706.

Huang, T., Kerstetter, R.A. and Irish, V.F. (2014) APUM23, a PUF family protein, functions in leaf development and organ polarity in Arabidopsis. *J. Exp. Bot.* **65**, 1181–1191.

Huh, S.U., Kim, M.J. and Paek, K.H. (2013) Arabidopsis Pumilio protein APUM5 suppresses *Cucumber mosaic virus* infection via direct binding of viral RNAs. *Proc. Natl Acad. Sci. USA* **110**, 779–784.

Ingouff, M., Hamamura, Y., Gourgues, M., Higashiyama, T. and Berger, F. (2007) Distinct dynamics of HISTONE3 variants between the two fertilization products in plants. *Curr. Biol.* **17**, 1032–1037.

Kiss, D.L. and Andrulis, E.D. (2011) The exozyme model: a continuum of functionally distinct complexes. *RNA*, **17**, 1–13.

Kumakura, N., Otsuki, H., Tsuzuki, M., Takeda, A. and Watanabe, Y. (2013) *Arabidopsis* AtRRP44A is the functional homolog of Rrp44/Dis3, an

exosome component, is essential for viability and is required for RNA processing and degradation. *PLoS ONE*, **8**, e79219.

Kuo, M.W., Wang, S.H., Chang, J.C., Chang, C.H., Huang, L.J., Lin, H.H., Yu, A.L., Li, W.H. and Yu, J. (2009) A novel *puf-A* gene predicted from evolutionary analysis is involved in the development of eyes and primordial germ-cells. *PLoS ONE*, **4**, e4980.

Lahmy, S., Guilleminot, J., Cheng, C.M., Bechtold, N., Albert, S., Pelletier, G., Delseny, M. and Devic, M. (2004) *DOMINO1*, a member of a small plant-specific gene family, encodes a protein essential for nuclear and nucleolar functions. *Plant J.* **39**, 809–820.

Lange, H., Holec, S., Cognat, V., Pieuchot, L., Le Ret, M., Canaday, J. and Gagliardi, D. (2008) Degradation of a polyadenylated rRNA maturation by-product involves one of the three RRP6-like proteins in *Arabidopsis thaliana*. *Mol. Cell. Biol.* **28**, 3038–3044.

Lange, H., Sement, F.M. and Gagliardi, D. (2011) MTR4, a putative RNA helicase and exosome co-factor, is required for proper rRNA biogenesis and development in *Arabidopsis thaliana*. *Plant J.* **68**, 51–63.

Li, Y., Lee, K.K., Walsh, S., Smith, C., Hadingham, S., Sorefan, K., Cawley, G. and Bevan, M.W. (2006) Establishing glucose- and ABA-regulated transcription networks in *Arabidopsis* by microarray analysis and promoter classification using a Relevance Vector Machine. *Genome Res.* **16**, 414–427.

Li, N., Yuan, L., Liu, N., Shi, D., Li, X., Tang, Z., Liu, J., Sundaresan, V. and Yang, W.C. (2009) *SLOW WALKER2*, a NOC1/MAK21 homologue, is essential for coordinated cell cycle progression during female gametophyte development in Arabidopsis. *Plant Physiol.* **151**, 1486–1497.

Li, H.J., Liu, N.Y., Shi, D.Q., Liu, J. and Yang, W.C. (2010) YAO is a nucleolar WD40-repeat protein critical for embryogenesis and gametogenesis in Arabidopsis. *BMC Plant Biol.* **10**, 169.

Liu, M., Shi, D.Q., Yuan, L., Liu, J. and Yang, W.C. (2010) *SLOW WALKER3*, encoding a putative DEAD-box RNA helicase, is essential for female gametogenesis in Arabidopsis. *J. Integr. Plant Biol.* **52**, 817–828.

Lorkovic, Z.J. (2009) Role of plant RNA-binding proteins in development, stress response and genome organization. *Trends Plant Sci.* **14**, 229–236.

Luo, M., Dennis, E.S., Berger, F., Peacock, W.J. and Chaudhury, A. (2005) *MINISEED3* (*MINI3*), a *WRKY* family gene, and *HAIKU2* (*IKU2*), a leucine-rich repeat (*LRR*) *KINASE* gene, are regulators of seed size in Arabidopsis. *Proc. Natl Acad. Sci. USA* **102**, 17531–17536.

Marondedze, C., Thomas, L., Serrano, N.L., Lilley, K.S. and Gehring, C. (2016) The RNA-binding protein repertoire of *Arabidopsis thaliana*. *Sci. Rep.* **6**, 29766.

Matias-Hernandez, L., Battaglia, R., Galbiati, F., Rubes, M., Eichenberger, C., Grossniklaus, U., Kater, M.M. and Colombo, L. (2010) *VERDANDI* is a direct target of the MADS domain ovule identity complex and affects embryo sac differentiation in *Arabidopsis*. *Plant Cell*, **22**, 1702–1715.

Mayer, U., Buttner, G. and Jürgens, G. (1993) Apical-basal pattern formation in the *Arabidopsis* embryo: studies on the role of the gnom gene. *Development*, **117**, 149–162.

Miller, M.A. and Olivas, W.M. (2011) Roles of Puf proteins in mRNA degradation and translation. *Wiley Interdiscip. Rev. RNA*, **2**, 471–492.

Mitchell, P., Petfalski, E., Shevchenko, A., Mann, M. and Tollervey, D. (1997) The exosome: a conserved eukaryotic RNA processing complex containing multiple 3′→5′ exoribonucleases. *Cell*, **91**, 457–466.

Möller, B. and Weijers, D. (2009) Auxin control of embryo patterning. *Cold Spring Harb. Perspect. Biol.* **1**, a001545.

Naudin, C., Hattabi, A., Michelet, F. *et al.* (2017) PUMILIO/FOXP1 signaling drives expansion of hematopoietic stem/progenitor and leukemia cells. *Blood*, **129**, 2493–2506.

Oh, S.A., Park, K.S., Twell, D. and Park, S.K. (2010) The *SIDECAR POLLEN* gene encodes a microspore-specific LOB/AS2 domain protein required for the correct timing and orientation of asymmetric cell division. *Plant J.* **64**, 839–850.

Okita, T.W. and Choi, S.-B. (2002) mRNA localization in plants: targeting to the cell's cortical region and beyond. *Curr. Opin. Plant Biol.* **5**, 553–559.

Petrasek, J. and Friml, J. (2009) Auxin transport routes in plant development. *Development*, **136**, 2675–2688.

Piekna-Przybylska, D., Decatur, W.A. and Fournier, M.J. (2008) The 3D rRNA modification maps database: with interactive tools for ribosome analysis. *Nucleic Acids Res.* **36**, D178–D183.

Qiu, C., McCann, K.L., Wine, R.N., Baserga, S.J. and Hall, T.M. (2014) A divergent Pumilio repeat protein family for pre-rRNA processing and mRNA localization. *Proc. Natl Acad. Sci. USA* **111**, 18554–18559.

Quenault, T., Lithgow, T. and Traven, A. (2011) PUF proteins: repression, activation and mRNA localization. *Trends Cell Biol.* **21**, 104–112.

Scheer, H., Zuber, H., De Almeida, C. and Gagliardi, D. (2016) Uridylation earmarks mRNAs for degradation. . . and more. *Trends Genet.* **32**, 607–619.

Shi, D.Q., Liu, J., Xiang, Y.H., Ye, D., Sundaresan, V. and Yang, W.C. (2005) *SLOW WALKER1*, essential for gametogenesis in Arabidopsis, encodes a WD40 protein involved in 18S ribosomal RNA biogenesis. *Plant Cell*, **17**, 2340–2354.

Sikorski, P.J., Zuber, H., Philippe, L., Sement, F.M., Canaday, J., Kufel, J., Gagliardi, D. and Lange, H. (2015) Distinct 18S rRNA precursors are targets of the exosome complex, the exoribonuclease RRP6L2 and the terminal nucleotidyltransferase TRL in *Arabidopsis thaliana*. *Plant J.* **83**, 991–1004.

Spassov, D.S. and Jurecic, R. (2003) The PUF family of RNA-binding proteins: does evolutionarily conserved structure equal conserved function? *IUBMB Life*, **55**, 359–366.

Steffen, J.G., Kang, I.H., Macfarlane, J. and Drews, G.N. (2007) Identification of genes expressed in the Arabidopsis female gametophyte. *Plant J.* **51**, 281–292.

Tam, P.P., Barrette-Ng, I.H., Simon, D.M., Tam, M.W., Ang, A.L. and Muench, D.G. (2010) The Puf family of RNA-binding proteins in plants: phylogeny, structural modeling, activity and subcellular localization. *BMC Plant Biol.* **10**, 44.

Wang, X., McLachlan, J., Zamore, P.D. and Hall, T.M. (2002) Modular recognition of RNA by a human pumilio-homology domain. *Cell*, **110**, 501–512.

Wang, D., Zhang, C., Hearn, D.J., Kang, I.H., Punwani, J.A., Skaggs, M.I., Drews, G.N., Schumaker, K.S. and Yadegari, R. (2010) Identification of transcription-factor genes expressed in the Arabidopsis female gametophyte. *BMC Plant Biol.* **10**, 110.

Weis, B.L., Kovacevic, J., Missbach, S. and Schleiff, E. (2015a) Plant-specific features of ribosome biogenesis. *Trends Plant Sci.* **20**, 729–740.

Weis, B.L., Palm, D., Missbach, S., Bohnsack, M.T. and Schleiff, E. (2015b) atBRX1-1 and atBRX1-2 are involved in an alternative rRNA processing pathway in *Arabidopsis thaliana*. *RNA*, **21**, 415–425.

Wharton, R.P., Sonoda, J., Lee, T., Patterson, M. and Murata, Y. (1998) The Pumilio RNA-binding domain is also a translational regulator. *Mol. Cell*, **1**, 863–872.

Xiang, Y., Nakabayashi, K., Ding, J., He, F., Bentsink, L. and Soppe, W.J. (2014) *Reduced Dormancy5* encodes a protein phosphatase 2C that is required for seed dormancy in *Arabidopsis*. *Plant Cell*, **26**, 4362–4375.

Yosefzon, Y., Koh, Y.Y., Chritton, J.J. *et al.* (2011) Divergent RNA binding specificity of yeast Puf2p. *RNA*, **17**, 1479–1488.

Zamore, P.D., Williamson, J.R. and Lehmann, R. (1997) The Pumilio protein binds RNA through a conserved domain that defines a new class of RNA-binding proteins. *RNA*, **3**, 1421–1433.

Zanchin, N.I. and Goldfarb, D.S. (1999) The exosome subunit Rrp43p is required for the efficient maturation of 5.8S, 18S and 25S rRNA. *Nucleic Acids Res.* **27**, 1283–1288.

Zhang, C. and Muench, D.G. (2015) A nucleolar PUF RNA-binding protein with specificity for a unique RNA sequence. *J. Biol. Chem.* **290**, 30108–30118.

